






Cite this: *Environ. Sci.: Water Res. Technol.*, 2022, **8**, 1675

Removal of nanoparticles (both inorganic nanoparticles and nanoplastics) in drinking water treatment – coagulation/flocculation/sedimentation, and sand/granular activated carbon filtration†

C. H. M. Hofman-Caris, ^{‡ab} P. S. Bäuerlein, ^{‡a} W. G. Siegers,^a S. M. Mintenig,^{§ac} R. Messina,^a S. C. Dekker,^{§c} Ch. Bertelkamp,^{§ad} E. R. Cornelissen^{ae} and A. P. van Wezel ^f

Nanoparticles, such as metallic ones like Ag, Au and TiO₂ as well as nanoplastics, are applied in or emitted by a wide variety of products or stem from degradation. Consequently, they end up in surface water, which is used as a source for drinking water production. This study investigated the removal of such nanoparticles by conventional water treatment processes Coagulation/flocculation/sedimentation (CFS), rapid sand filtration (RSF) and filtration over granular activated carbon (GAC) in different water matrices. In principle these processes appeared to remove the majority of nanoparticles. Lab-scale batch experiments confirmed that CSF may also be effective. In this study Au and Ag nanoparticles with a negative surface charge were used, as well as nanoplastics varying in size (50 and 200 nm) and surface charge (neutral and negative). It was found that the presence of negatively charged NOM has an adverse effect on inorganic nanoparticle removal, whereas the presence of cations like Ca²⁺ and Mg²⁺ is essential for good removal. In column experiments it was shown that the mechanism of nanoparticle removal by sand filtration differs from that by GAC filtration. A comparison of demineralized water and natural water showed that in sand filters the water matrix and the presence of biomass on the particles have a positive effect on the removal rate, whereas for GAC filters they have a distinct negative effect. Furthermore, larger nanoplastics (200 nm) were most efficiently removed by CFS, whereas smaller nanoplastics (50 nm) were removed better by GAC filtration. For smaller nanoparticles charge interactions play a more important role than for larger nanoparticles.

Received 31st March 2022,
Accepted 13th May 2022

DOI: 10.1039/d2ew00226d

rsc.li/es-water

Water impact

Both sand and GAC filtration can remove nanoplastics and nanoparticles from water to a certain extent. Coagulation can effectively remove nanoparticles in the presence of bivalent cations and a low concentration of NOM.

^a KWR Water Research Institute, The Netherlands.

E-mail: roberta.hofman-caris@kwrwater.nl

^b Wageningen University and Research, The Netherlands

^c Copernicus Institute of Sustainable Development, Utrecht University, The Netherlands

^d Waternet, Amsterdam, The Netherlands

^e Particle and Interfacial Technology Group, Department of Green Chemistry and Technology Faculty of Bioscience Engineering, Ghent University, Coupure Links 653, B-9000 Ghent, Belgium

^f Institute for Biodiversity and Ecosystem Dynamics, University of Amsterdam, The Netherlands

† Electronic supplementary information (ESI) available. See DOI: <https://doi.org/10.1039/d2ew00226d>

‡ These authors contributed equally.

§ Current address Wageningen University and Research, The Netherlands.

Introduction

The use of nanomaterials (defined as materials having three dimensions <100 nm) in industrial, consumer, and medical products, and in fertilizers or plant protection products has strongly increased over the past few years.¹ Via among others wastewater effluent and sewage sludge these materials enter the environment,² and this is cause for concern.³ Nanoparticles may affect the entire organ system, adsorb and transport other harmful chemicals and enable them to enter into organisms.⁴ Kaegi and Voegelin⁵ studied the removal of inorganic nanoparticles (nAg and nAu) from wastewater by activated sludge and concluded that the major part is

removed. According to Westerhoff and Atkinson⁶ 90% of the nanoparticles can be removed by wastewater treatment plants (WWTPs). However, as the total number of nanoparticles in a WWTP is very high, the remaining 10% still is a significant amount. As a result Sousa and Ribau Teixeira⁴ showed that wastewater effluents usually can be considered as one of the most significant point sources of nanoparticles in surface waters.

Dissolution and aggregation are important processes in relation to the possible toxic effects of nanoparticles.⁷ The presence and structure of natural organic matter (NOM) certainly plays an important role in the behavior and effects of nanoparticles.⁸ NOM may increase the stability of nanoparticles in an aqueous environment, facilitating their distribution in *e.g.* surface waters, whereas, on the other hand, it may lower their toxicity. Angel and Batley⁹ studied the impact of size on the fate and toxicity of silver nanoparticles in aquatic systems. They found that dissolution, and thus toxicity, of silver from nanoparticles can be reduced by the presence of NOM. However, as it often was difficult to determine exact loads of nanoparticles in the environment, it was also tried to obtain more information on their occurrence and effects by applying modelling.^{2,10,11} In recent years it has become possible to measure the concentrations of nanoparticles. They have been detected in *e.g.* sources for drinking water and in tap water at concentrations in the ng L^{-1} to $\mu\text{g L}^{-1}$ range.^{4,12,13} Peters and van Bommel¹³ measured the concentrations of Ag, CeO_2 and TiO_2 particles in the rivers Meuse and IJssel, and concluded that these concentrations are in good accordance with predicted concentrations. In the Meuse nano Ag concentrations ranged from 0.3–6.6 ng L^{-1} , or 1×10^7 to 2.5×10^7 particles per L, and in the IJssel from 0.3–2.5 ng L^{-1} or 0.5×10^7 – 3.5×10^7 particles per L. The average size of the particles was 15 nm in both rivers. Markus and Parsons¹⁴ found that nanoparticles contribute 5–20% to the total loads of zinc and titanium in the Dutch catchment areas of the Meuse and the Rhine, and for silver the contribution is about 3%. In a previous study we were able to show that nanoparticles, such as nano silver (nAg) and nano gold (nAu), are present in the Dutch water cycle.¹⁵ nAg is applied in for example healthcare products and textiles, and nAu in electronic equipment and catalysts. As this surface water is a source for drinking water, it is important to understand how well these nanoparticles can be removed by different treatment processes.

Retention of nanoparticles by drinking water treatment processes is important, but fairly unknown due to the high analytical challenges. Although Westerhoff and Atkinson⁶ concluded that engineered nanoparticles will be effectively removed by filtration processes in drinking water treatment, designed to remove natural nanoparticles, other authors did detect the presence of nanoparticles in tap water, although in significantly lower concentrations than in surface water.⁴ This may be caused by the fact that engineered nanoparticles have different (adsorption) properties compared to natural

nanoparticles.⁴ CFS (coagulation–flocculation–sedimentation) reduces the water turbidity by adding a coagulant to initiate the aggregation of particles smaller than 1 μm into flocs and that way enabling them to settle.¹⁶ According to Donovan and Adams¹² conventional drinking water treatment (applying lime softening, alum coagulation, filtration and disinfection) seemed to nearly completely remove Ag, Au and Ti-containing nanoparticles, although Abbott Chalew and Ajmani¹⁷ concluded that some metal nanoparticles could still be observed in tap water. Different treatment processes give different results. Membrane filtration (MF, NF, UF) can be very effective for the removal of nanoparticles, although some breakthrough may occur. After microfiltration breakthrough was 1–45%, and after ultrafiltration 0–2%. Sousa and Ribau Teixeira⁴ present an overview of coagulation/flocculation experiments that have been described in literature, and show that the efficiency rates are highly variable. They depend on the type of nanoparticles, the dosage and types of coagulant and/or flocculant applied, mixing conditions and the composition of the water matrix (*e.g.* the composition and concentration of NOM). The optimum alum dose for coagulation processes depends on the type of nanoparticles that will have to be removed (*e.g.* ZnO , TiO_2 or Ag). For Ag particles only 2–20% could be removed. Sand filters may remove uncoated nanoparticles to some extent, but appeared to be less effective for coated particles. However, in practice sand filtration will often be preceded by coagulation/flocculation, which may increase the efficiency. Application of powdered activated carbon showed varying effectiveness in the removal of nanoparticles. To the best of the authors knowledge, the removal of nanoparticles with granular activated carbon filtration has not been investigated yet.

A category of nanoparticles that recently gets more attention is nanoplastics. The widespread occurrence of microplastics in freshwater ecosystems has been confirmed by numerous studies,^{18–20} but knowledge on occurrence and removal efficiency for nanoplastics is still scarce. However, it has been shown that they are present in cosmetics,²¹ that they can be formed as a result of UV exposure,²² and that they are present in the environment.^{23,24} Pivokonský and Pivokonská²⁵ determined that full-scale drinking water treatment plants (DWTP) applying different techniques removed, on average, 73% of the microplastics present in surface water. Wang and Lin²⁶ quantified the removal of microplastics down to 1 μm between treatment steps in a DWTP. Microplastics removal was highest for CFS, and the subsequently applied rapid sand filtration removed all microplastics $>10 \mu\text{m}$, but only 30% of the smaller microplastics. This is in accordance with laboratory experiments studying transport mechanisms in porous media. While Hou and Xu²⁷ reported that 35% of 45 μm sized microplastics migrated through a sand column, this increased to approximately 80% for smaller microplastics and nanoplastics.^{28–30} Because of their small size, nanoplastics are likely the most hazardous plastic items.^{18,31}

The removal of nanoparticles by means of CSF has been described in literature,^{32–38} but studies on sand or GAC (granular activated carbon) filtration are limited. Ramirez Arenas *et al.*^{39–41} studied the effect of coagulation and filtration over sand or GAC filters on the removal of polystyrene nanoparticles (90 ± 7 nm). The efficiency of the CSF process strongly depends on parameters, such as the type of nanoparticles, composition and concentration of NOM, ions, pH, and type and dosing of the coagulant. Therefore, it was unclear how filtration over *e.g.* sand or GAC could contribute to the removal of nanoparticles during drinking water treatment. Especially as it is becoming increasingly clear that not only metal but also plastic nanoparticles may be present in sources for drinking water, it is important to understand the behavior of different types of nanoparticles in drinking water treatment processes. Where Ramirez Arenas *et al.* applied nanoplastics of about 90 nm, here nanoplastics of 50 and 200 nm were applied.

The experiments described in this study provide insight in the extent that both materials (sand/GAC) can contribute to overall nanoparticle removal, the separate contribution of the water matrix and the filter medium (effect of biomass), and the effect of influent concentration. This is the first time that the effects of both CSF and sand/GAC filtration on the removal of both inorganic and plastic nanoparticles in drinking water are described as a function of the concentration of the particles, their composition and charge. The word ‘nanoparticles’ (abbreviated as NPs) in this study refers to both inorganic NPs and nanoplastics. If a distinction has to be made, for inorganic NPs either ‘inorganic NPs’ or nAu/nAg are used. For nanoplastics always ‘nanoplastics’ is used.

Chemicals and methods

Nanoparticles

nAg with an average size of 48 nm and nAu with an average diameter of 51 nm (both citrate capped) were obtained from Nanocomposit Europe, Prague. Monodispersed polystyrene spheres (Polyscience Inc., US) were used that differed in size (50 and 200 nm) and functionalized groups. The surfaces of the nanoplastics were either plain (uncharged) or modified with carboxyl groups (COOH) which commonly occur on weathered plastics³⁰ and by which the latter were more negatively charged.

Analyses

Inorganic nanoparticles (nAu, nAg) were analyzed using an ICP-MS type X Series II (Thermo Fisher, Scientific, Breda) in single particles mode with a dwell time of 10 ms.^{42–44} The system was calibrated with citrate-capped nAg (20 ng L^{-1}) and nAu (51 ng L^{-1}) dispersions. The average size of these particles was between 48 and 50 nm (see Fig. SI 1 and SI 2†). The stability of the signal was checked using an internal standard ($10 \mu\text{g L}^{-1}$ Rh in 2% HNO_3) and the signal intensity of nAu and nAg was corrected with the internal standard to

compensate for eventual signal intensity changes. Samples were analyzed within one hour.

Nanoplastics concentrations were determined using UV-VIS spectrophotometry (Thermo Spectronic Unicam UV-500, US) as the concentration of polystyrene was proportional to the UV absorption at 229 nm (Fig. SI 3†). Samples from the CFS tests were subjected to ultrasonic treatment prior to measurements to break up aggregates, and samples taken during the filtration experiments were analysed within two hours after finishing the experiments.

Prior to the experiments ICP-MS was applied to determine whether the inorganic NPs had been well dispersed, and to quantify the number of inorganic NPs.

ATP measurements were carried out according to the procedure described by Timmers *et al.*⁴²

Coagulation–flocculation–sedimentation (CFS) experiments

CSF Experiments were carried out twice in a setup with six identical Perspex 2 L beakers, containing baffles to create ideal mixing profiles with known g-forces during mixing and the formation of flocs. These beakers were filled with 1.8 L of water (Table 1) to which NPs had been added. The solution firstly was stirred at a speed of 400 rpm for 10 s, followed by addition of NaOH or HCl to adjust the pH. Again the solution was stirred at 400 rpm for 10 s. Then FeCl_3 (0, 0.5, 1.0 and 1.5 mg L^{-1}) was dosed and mixed during 10 s at 400 rpm. Subsequently, stirring speed was reduced to 70 rpm for floc formation during 15 min. Finally, mixing was stopped and sedimentation took place during 30 min. Chemicals were dosed with compressed air. In pre-tests turbidity and TOC reduction were determined for two different coagulant doses and nanoplastics (Fig. SI 4†). Requirements for the production of drinking water were reached within 30 min.⁴³ Raw water from the Lek was used – a tributary of the Rhine and used as a source of drinking water by Waternet.

For the nanoplastics FeCl_3 concentrations of 12 and 18 mg FeCl_3/L were applied which is similar to concentrations in full scale DWTPs^{16,44,45} and to a previous investigation.³² In pre-tests it was confirmed that these Fe concentrations sufficiently reduce the water turbidity (2100Q PorTable 6-Turbidimeter, HACH, US) and TOC (LCK380, HACH, US). After adding NPs to the surface water (10 mg L^{-1} , admixed for 30 minutes at 60 rpm) the actual CFS started. Addition of chemicals and mixing schedule applied were identical to the procedure for inorganic NPs. Using a syringe the supernatant (2 cm below the water surface) was sampled at 0, 20, 60 and 120 minutes.

For inorganic NPs the effect of water matrix composition was studied by pre-treating the water an anionic exchange resin (Lanxess Lewatit VPOC 1072, which removes a significant part of NOM) or a cationic exchange resin (for the removal of Ca^{2+} and Mg^{2+} ions; Lanxess Lewatit Monoplus S108) at pH = 8. Results were compared to results obtained in demineralized (demi) water. In this way the effect of NOM, Ca^{2+} and Mg^{2+} on nAu removal was studied. Several doses of

Table 1 Water quality data for CFS experiments

	Demineralized water	Lek untreated	Lek after cation exchange	Lek after anion exchange
pH	7.31	7.99	8.22	7.53
EGV ($\mu\text{S cm}^{-1}$)	0.76	434	446	492
Turbidity (FTU)	0.2	21.0	15.0	7.5
TOC (mg L^{-1})	<0.20	3.5	3.4	1.2
Ca^{2+} (mg L^{-1})	<1.0	61	1.5	58
Mg^{2+} (mg L^{-1})	<1.0	9.4	<1.0	8.9
Remarks	No flocculation or sedimentation observed	Clear flocculation and sedimentation	No clear flocculation, hardly any sedimentation	Clear flocculation and sedimentation

FeCl_3 (0, 0.5, 1 and 1.5 $\text{mg FeCl}_3/\text{L}$) were tested. Furthermore, to determine the effect of pH on nAu removal, experiments were carried out at pH values of 5, 6, 7, 8, 9 and 10, using NaOH or HCl. As a coagulant 3 mg L^{-1} FeCl_3 was applied (this is lower than in the other study, as in this case the water was pretreated by IEX). The water matrix parameters are shown in Table 1.

Column experiments

Column experiments were carried out to study the removal efficiency of both sand and GAC filters for nAu, nAg and nanoplastics. Columns with a length of 1 m and a diameter of 3.5 cm were filled with clean or pre-loaded sand (bedheight 70–83 cm) or GAC (20–99 cm). For the nAu and nAg experiments, GAC was obtained from Norit (ROW Supra 0.8), also the pre-loaded coal for nAu/nAg removal was Norit ROW Supra 0.8 and obtained from Waternet (life time 1600 days at the Leiduin drinking water treatment plant). Sand for the nAu/nAg experiments was obtained from Acqua Silica® (Kremer zand en grind BV, The Netherlands) (0.8–1.25 mm). The pre-loaded sand was the same type of sand, but obtained from the Waternet rapid sand filters at Nieuwegein (pretreatment of the drinking water process). For the nanoplastic experiments the clean sand, and the pre-loaded GAC were used, both in combination with the pretreated water from the Lek canal in Nieuwegein.

First water was added to the columns, and then 3–4 cm layers of sand were added. GAC was applied in a slurry in demineralized water, to prevent air entrapment between GAC particles. Dust was removed from the GAC by washing with demineralized water, and the virgin GAC was heated to about 60 °C to fill the GAC pores with water. The pre-loaded sand was only rinsed with water from Leiduin.

For column experiments with nAu/nAg the following procedure was applied. For the sand columns pretreated (CFS and rapid sand filtration; WRK) water from the river Lek in Nieuwegein was used. Experiments were carried out within four days after sampling (as also ATP measurements were carried out to check the presence of microbiological activity in the water, and the effect of the experiments on this

activity). GAC experiments (with virgin and pre-loaded GAC) were carried out with water after dune filtration in Leiduin, simulating the full-scale GAC filters at this production location. A schematic diagram of the experimental set-up is shown in Fig. 1. Before elution nanoparticles were continuously fed to the columns. By comparing nAu/nAg removal in GAC and sand columns, insight is gained in the capacity of these filter media to remove these particles. Comparing the column fed with demineralized water to Leiduin water/WRK water provides insight in the contribution of the water matrix to overall nAu/nAg removal. Similarly, comparing the column filled with virgin GAC/sand to the pre-loaded GAC/sand (both fed with Leiduin/WRK water) provides insight in the role of biomass on the overall particle removal. Finally comparing low doses of nAg/nAu to high doses elucidates the effect of influent concentration on the removal. This aspect has only been investigated for sand columns (Table 3), high dosing (influent concentrations) was used for the GAC filters.

Tracer experiments were carried out to determine the dispersion coefficient and the porosity, and to check that no short circuit currents occurred. A NaCl solution (10 g L^{-1}) was added to the column until the influent and effluent concentrations became identical, which was checked by measuring the conductivity of the water. Breakthrough curves were fitted with the advection-dispersion equation⁴⁶ (see ESI†). The bed porosity of clean sand was 38%, the bed porosity of pre-loaded sand was measured to be 42%.

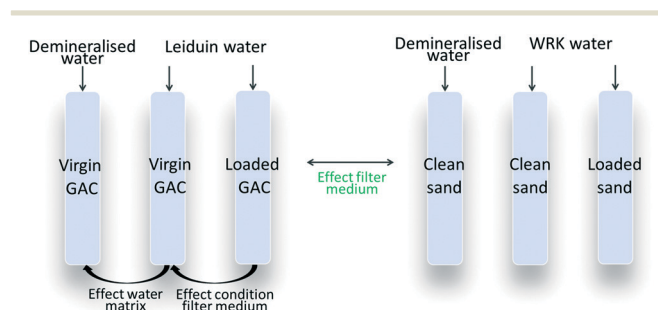
**Fig. 1** Schematic diagram of the column experiments.

Table 2 Porosity data of GAC in the nAu/nAg experiments

Type of GAC	V_{tot} (cm ³ g ⁻¹)	V_{intra} (cm ³ g ⁻¹)	V_{inter} (cm ³ g ⁻¹)	Bulk density (g cm ⁻³)	Bed porosity (%)
Virgin GAC	1.50	1.06	0.44	0.38	17
Pre-loaded GAC	1.15	0.66	0.49	0.45	22

Table 3 Experimental conditions of column experiments with nAg en nAu. HD = high dose of nAu/nAg; LD = low dose of nAu/nAg

Filtermedium	Type of water	Dose	Concentration nAu/nAg (total amount of particles)
Clean sand	Demineralsed water	HD	$9.89 \times 10^8 / -$
Clean sand	WRK	HD	$9.23 \times 10^8 (\pm 5.38 \times 10^7) / 2.23 \times 10^9 (\pm 4.45 \times 10^7)$
Pre-loaded sand	WRK	HD	$6.40 \times 10^8 (\pm 6.52 \times 10^7) / 1.49 \times 10^9 (\pm 7.16 \times 10^7)$
Clean sand	WRK	LD	$1.56 \times 10^8 (\pm 1.08 \times 10^7) / 3.53 \times 10^8 (\pm 1.64 \times 10^7)$
Pre-loaded sand	WRK	LD	$1.75 \times 10^8 (\pm 7.74 \times 10^6) / 3.34 \times 10^8 (\pm 3.12 \times 10^7)$
Virgin GAC	Demineralsed water	HD	$8.04 \times 10^8 / 1.37 \times 10^9$
Virgin GAC	Leiduin water	HD	$7.97 \times 10^8 / 1.60 \times 10^9$
Pre-loaded GAC	Leiduin water	HD	$7.46 \times 10^8 / 1.42 \times 10^9$

Porosity of the GAC was measured with mercury intrusion porosimetry, nitrogen adsorption (BET) and helium pycnometry. Bulk density was measured using a measuring cylinder. According to the supplier, the bulk density should be between 0.35 and 0.45 g cm⁻³. From these data bed porosity was calculated, as shown in Table 2.

For the calculations two size characterizations were applied: d_{10} (90% of the particles has a larger diameter) and d_{50} (50% of the particles has a larger diameter). The characterizations of the filters applied are shown in the ESI† (Tables SI1 and SI2).

For the nanoplastics first water with nanoplastics (2 mg L⁻¹) was continuously added to the column, and subsequently the columns were eluted using the same water without nanoplastics added. Assuming a density of polystyrene of about 1 g cm⁻³, this amounts to a concentration of 3.06×10^{13} particles per L for particles with a diameter of 50 nm, and 4.77×10^{11} particles per L for nanoplastics with a diameter of 200 nm. In all cases breakthrough curves were generated.

During the experiment the following water quality parameters were measured in the feed and treated water: UV₂₅₄, Ca²⁺, Mg²⁺, DOC, turbidity, nitrate, suspended solids, pH, temperature and conductivity. Results are shown in the ESI† (Tables SI3–SI6), just as ATP-measurement data (Table SI7†), which are an indication for the active biomass present.

Modelling of particles removal

The behavior of particles in a filter bed can be described by the colloid filtration theory (CFT).^{47–49} Modelling equations are shown in detail in the ESI.† The collector efficiency η_0 describes the efficiency of NP-delivery to the filter surfaces.⁵⁰ Together with the attachment efficiency α , indicating how efficiently particles stick to the filter material after a collision, the removal efficiency can be calculated. These parameters enable comparing the retention of different NPs for different filter materials.

H_0 is the sum of individual transport mechanisms (eqn (1)):

$$\eta_0 = \eta_D + \eta_I + \eta_G \quad (1)$$

In which η_D is transport efficiency by diffusion, η_I is transport efficiency by interception and η_G is transport efficiency due to gravity. Larger colloids typically have a larger η_I and η_G , while Brownian motion, and thus η_D , is larger for smaller colloids.⁵⁰ Using η_0 , the attachment efficiency α was determined which indicates the fraction of contacts needed for a colloid to attach to the filter material (eqn (2)).

$$\alpha_c = -\frac{2}{3} \times \frac{d_c}{(1-f)L\eta_0} \times \ln \frac{C}{C_0} \quad (2)$$

in which:

d_c = median diameter of the used filter material [m].

f = porosity [-].

L = length of the filter bed [m].

C = effluent concentration [mg L⁻¹].

C_0 = dosing NPs concentration [mg L⁻¹].

Lastly, the single-collector removal efficiency (η) is calculated which expresses the capacity of the filter material to trap NP. It is the product of the attachment efficiency (α_c) and the single-collector contact efficiency (η_0), eqn (3).

$$H = \alpha_c \times \eta_0 \quad (3)$$

The porosity of a GAC filter consists of a combination of inter particle bed porosity and the internal porosity of the GAC granules. To calculate the collision frequency (α_c) the inter particle porosity was estimated from mercury intrusion porosimetry, nitrogen adsorption (BET) and helium pycnometry. Bed height (L) is known. D is the dispersion coefficient, d is the particle diameter. 90% of all particles has a diameter larger than d_{10} , and 50% has a diameter larger than d_{50} . Both d_{10} or d_{50} can be determined from sieving fractions of the filter material. In literature there still is a

discussion on the question whether d_{10} or d_{50} should be applied, and therefore the collision frequency α_c was determined for both diameters in case of the inorganic NPs.

Results and discussion

CSF experiments.

Batch experiments were used to determine the effects of ions (Ca^{2+} and Mg^{2+}) and NOM on the removal of the citrate capped nAu (Table 4). Ca^{2+} and Mg^{2+} were removed with a cationic exchange resin, whereas NOM was partly removed with an anionic exchange resin.

The data show no precipitation in the Demi water experiment. The absence of cations hampers the flocculation process. nAu is removed, however, the percentage is low. The highest removal (77%) is achieved in Lek water with a low NOM concentration. In untreated Lek water the highest removal is $57 \pm 2.6\%$. This indicates that the presence of bivalent cations is crucial for the formation of iron flakes that in turn stick to nAu. The lower removal of nAu from the untreated Lek water would suggest that NOM in some way interferes with the incorporation of nAu into the iron flakes. A possible explanation is that both nAu and humic acids are negatively charged, and may compete for the Fe^{3+} in the coagulant. Negatively charged particles are removed best with FeCl_3 .^{51–53} For both the untreated and the Lek water with low NOM content applies the higher the FeCl_3 concentration the higher the removal.

For a FeCl_3 -concentration of 1 mg L^{-1} a pH sweep was carried out in untreated Lek-water and the removal of nAu was monitored (Fig. 2). With increasing pH, the removal of nAu was increased. This is probably caused by the effect of pH on the zeta potential of the particles, as observed by Sun, Li.³³ The zeta potential will decrease and hence the negative charge becomes more pronounced. At pH values 5–6 nAu removal seems to be negligible.

During the experiments with the different nanoplastics, two coagulant dosages (12 and 18 mg L^{-1}) were tested. This resulted in a similar nanoplastics removal, increasing considerably with longer sedimentation times to an almost complete removal for both, the plain and carboxylated, larger nanoplastics after two hours (Fig. 3). However, contrary to our expectations, the negatively charged carboxylated nanoplastics were not systematically removed better than the plain nanoplastics. Instead, a considerable effect of nanoplastics size could be determined.

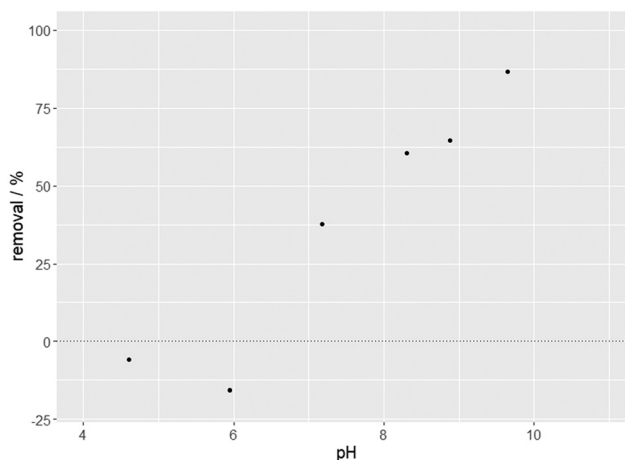


Fig. 2 Removal of nAu at different pH values. Addition of 1 mg L^{-1} of FeCl_3 . Experiments carried out in water from the Lek canal.

The settling of the bigger nanoplastics started immediately and in the supernatant a reduced nanoplastics concentration was determined already at the start of the experiments. After a settling time of 20 min, the bigger nanoplastics were removed by 83% (79–86%), while this was much lower for the smaller nanoplastics (6–47%). Also Zhang *et al.*⁴⁵ reported very low removal rates (2–13%) for plastic particles between 0.18–125 μm . The authors hypothesized that this was caused by the microplastics generally low settle ability, and a relatively large size by which they were not enmeshed in the formed flakes. As discussed previously, the floc formation depends strongly on other factors (*e.g.* water pH, surface charges, kinetic energy from mixing, sedimentation time or coagulant concentration) as well as operational conditions (*e.g.* sedimentation time and mixing energy). According to previous research,⁵¹ such differences could thus be an explanation for the contradictory results.

The results of the current study are similar to removal efficiencies determined in laboratory-scale experiments for other nano-sized particles. Removal efficiencies of approximately 80% for nAg, of more than 90% for nTiO₂ particles¹⁷ and of more than 80% for nC60 fullerenes (Floris 2017)^{32,37} were reported. Similarly, Lapointe *et al.* (2020)⁵⁸ determined removal rates of around 80% for smaller microplastics (15 and 140 μm) for which settling started instantly and for which removal was highest for weathered microplastics. The authors

Table 4 Effect of water matrix on nAu removal (%) during CFS (coagulant FeCl_3). Removal rates are in relation to the concentration in the water phase without any addition of FeCl_3 . All experiments were carried out twice, the values refer to the average values and the variation

Coagulant dose (mg Fe/L)/(FeCl_3/L)	nAu removal (%) from the water matrix			
	Demi water	Lek water	Lek water with low NOM concentration	Lek water with low Ca^{2+} and Mg^{2+} concentrations
0/0	0	0	0	0
0.5/1.45	2.6 ± 0.7	8.7 ± 4.6	35 ± 1.2	0
1.0/2.9	0	47 ± 0.3	66 ± 0.1	37 ± 26
1.5/4.35	0	57 ± 2.6	77 ± 0	8 ± 2.6

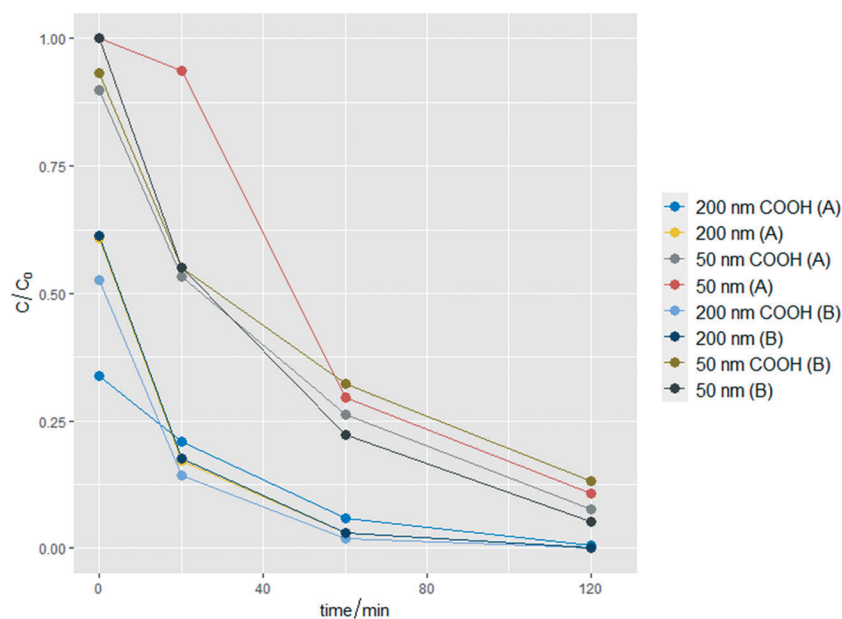


Fig. 3 Nanoplastics residual concentrations, determined in jar tests simulating coagulation–flocculation–sedimentation (CFS) for two iron chloride concentrations ($A = 12 \text{ mg L}^{-1}$, $B = 18 \text{ mg L}^{-1}$). Measured nanoplastics concentrations in the aqueous phase were normalized to initial nanoplastics concentrations.

attributed this to the irregular microplastics shape, or to the presence of hydroxyl and carboxylic groups. It might have rather been the shape, as the current findings could not support an effect of the modified NPs surfaces with carboxylic groups. However, further research is required to test this.

It has to be considered that the initial nanoplastics concentration of 10 mg L^{-1} is certainly too high to depict the environmental situation accurately, and was chosen due to analytical restrictions. Previous studies demonstrated a negligible effect of the initial concentration of nano-sized particles on their removal rates (Chalew *et al.* 2013b (ref. 17),

Table 5 Results of column experiments with nAu, nAg and nanoplastics; for detailed information on the parameters see the ESI† Unless stated otherwise, pretreated surface water was used. Characteristics based on d_{50}

Sample	Type of water	Particle	α_c	η
Clean sand, HD	River Lek in Nieuwegein	nAu	0.23	7.81×10^{-4}
Pre-loaded sand, HD	River Lek in Nieuwegein	nAg	0.27	9.58×10^{-4}
		nAu	0.55	1.67×10^{-3}
Clean sand, LD	River Lek in Nieuwegein	nAg	0.50	1.58×10^{-3}
		nAu	0.36	1.23×10^{-3}
Pre-loaded sand, LD	River Lek in Nieuwegein	nAg	0.34	1.23×10^{-3}
		nAu	0.48	1.43×10^{-3}
Virgin GAC, HD	After dune filtration in Leiduin	nAg	0.46	1.43×10^{-3}
		nAu	0.31	1.88×10^{-3}
Pre-loaded GAC, HD	After dune filtration in Leiduin	nAg	0.31	2.01×10^{-3}
		nAu	0.11	9.08×10^{-4}
Virgin GAC. Demineralized water, 20 cm column, HD	Demineralized water	nAg	0.12	1.02×10^{-3}
		nAu	0.39	2.40×10^{-3}
Virgin GAC. Demineralized water, 99 cm column, HD	Demineralized water	nAg	0.42	2.70×10^{-3}
		nAu	0.32	1.98×10^{-3}
Clean sand	Pretreated water from Lek Canal	Nanoplastics 200 COOH	0.22	1.9×10^{-4}
Clean sand	Pretreated water from Lek Canal	Nanoplastics 200 uncharged	0.47	4.1×10^{-4}
Clean sand	Pretreated water from Lek Canal	Nanoplastics 50 COOH	0.62	1.6×10^{-3}
Clean sand	Pretreated water from Lek Canal	Nanoplastics 50 uncharged	0.03	7.1×10^{-5}
Pre-loaded GAC	Pretreated water from Lek Canal	Nanoplastics 200 COOH	0.07	2.2×10^{-4}
Pre-loaded GAC	Pretreated water from Lek Canal	Nanoplastics 200 uncharged	0.28	9.0×10^{-4}
Pre-loaded GAC	Pretreated water from Lek Canal	Nanoplastics 50 COOH	0.10	9.4×10^{-4}
Pre-loaded GAC	Pretreated water from Lek Canal	Nanoplastics 50 uncharged	0.12	1.2×10^{-3}

Honda *et al.* 2014 (ref. 35)), however, further research might be needed to confirm this for nanoplastics specifically.

Column experiments

Breakthrough curves are shown in the ESI† (Fig. SI 5–SI 13 for nAu/nAg and Fig. SI 14 for nanoplastics). The characteristic parameters are shown in Table 5. α_c is the attachment efficiency, which reflects the number of collisions between a NP and a filter medium particle, that will result in deposition of the NP. The higher α_c the higher the NP removal by the filter material. η is the collector removal efficiency, which is the sum of transport due to diffusion, interception and gravity (see ESI† for more detailed information).

As the experiments were limited by the availability of the same water matrix and column material, for the experiments with nanoplastics ‘worst case’ conditions (clean sand and a pre-loaded GAC column) were applied. In this way the risks of the presence of NPs in sources of drinking water could be assessed.

During sand filtration the 50-COOH nanoplastics were removed by 63%, while lower particles removal rates (4–22%) were determined for the remaining three nanoplastics. These results are comparable to the ones from Chu, Li²⁸ and Zhao, Zhao²⁹ who reported that 20% of the smaller micro and nanoparticles were retained in a sand column.

For clean sand in the experiments with demineralized water no nAu removal could be measured ($\alpha_c \approx 0$) (see Fig. SI 5†). If clean sand is fed with pretreated surface water removal of particles improves (α_c increases). Table 5 shows that differences in behavior between nAg and nAu are very small or negligible. Applying a higher dose of NPs results in a lower value of α_c . This is reflected in the α_c value of the negatively charged 50 nm nanoplastics, but not for the plain, uncharged nanoplastics, indicating that surface charge may play a crucial role in this. For the 200 nm nanoplastics, however, the uncharged particles show an α_c value that is about twice as high as for the charged 200 nm plastics, although still significantly lower than for the 50 nm charged nanoplastics. This seems to indicate that for small NPs charge plays a more important role than for larger NPs. The sand grains ($d_{50} = 1016 \mu\text{m}$) formed pores considerably bigger than the used NPs. Using finer sand, Pradel, Hadri³⁰ concluded that larger nanoplastics (460 nm) deposited more easily than smaller nanoplastics (200 nm). Because smaller nanoparticles exhibit larger Brownian motion, their deposition due to diffusion is higher compared to bigger particles,⁵⁰ which is demonstrated in these experiments. Zhao, Zhao²⁹ reported that increasing the flow velocity or the ionic strength led to a higher microplastics deposition, and a thus higher attachment efficiency respectively. Pradel, Hadri³⁰ documented that the attachment efficiency largely depended on the sand grains.

Pradel, Hadri³⁰ also demonstrated that removal rates increased by one order of magnitude when injecting same-sized, but irregular shaped nanoplastics. Since environmental

nanoplastics are mostly a result of fragmentation and thus of irregular shape, higher removal efficiencies in full-scale DWTPs could be expected. The nAu and nAg results reported above show that the use of pre-loaded sand improves the retention, which may also be the case for nanoplastics. The present study could therefore be considered as a worse-case estimate for nanoplastics.

The removal of nAu/nAg over sand filters appeared to increase even further if pre-loaded sand from the full-scale treatment plant is used. This indicates that both the water matrix and possibly the presence of biomass in the sand, contribute to the removal of nanoparticles. This is in accordance with the findings on nanoplastics of Ramirez-Arenas *et al.*⁴⁰ An explanation might be that NOM from the surface water covers both the filter grains and the nanoparticles, thus facilitating sorption of nanoparticles to the filter material. Furthermore, nanoparticles may be entrapped by NOM, and the presence of cations ($\text{Ca}^{2+}/\text{Mg}^{2+}$) may also play a role, as was concluded from the previous section. These cations may bridge negatively charged sand grains and negatively charged nanoparticles. Further research will however be required to establish the exact removal mechanism. The positive contribution of biomass is in accordance with literature,^{54,55} where the authors suggest that the increased roughness of the sand grain surface and the decrease in pore volume as a result of the growth of biomass account for the higher removal rates observed. According to the ATP measurements (Table SI 7†) the concentration of cellular ATP significantly decreases during the filtration experiment with a high dose of inorganic NPs. This may be explained by the disinfecting properties of nAg.⁵⁶ With low doses of NPs no change in cellular ATP (cATP) content was observed.

Nanoplastics removal during GAC filtration appeared to be higher than during sand filtration. Approximately 60–70% of three types of initially added nanoplastics were retained in the column, except for the 200-COOH particles, from which only 20% were removed. Smaller nanoplastics (50 nm) were removed to a larger extent than the larger (200 nm) NP. This may be explained by the fact that GAC contains micro-, meso and macropores. The smaller the particle size, the better they may be adsorbed in the pores. In addition, for both sizes, the uncharged nanoplastics showed a higher removal than the carboxylated nanoplastics.

Most breakthrough curves of nAu/nAg reached a plateau almost instantly, which is in accordance with several other studies.^{28,30,50} However, in this case for GAC some different results were obtained. For virgin activated GAC α_c shows the highest value, similar to the values observed for clean sand with HD inorganic nanoparticles. Contrarily to what was observed with sand grains, in GAC α_c significantly decreases if pre-loaded GAC is applied, or if surface water is used instead of demi-water. This is in accordance with the results obtained for 200-COOH nanoplastics, but also for the 50 nm plain nanoplastics in both sand and GAC filtration. It is clear that the combination of water matrix and the presence of

biomass at the GAC surface has a negative effect on the nanoparticle removal. Other (colloidal) particles, NOM and possibly biomass might block the GAC pores, as a result of which it becomes more difficult to remove nanoparticles. As for sand, also for GAC further research will be required to establish the exact removal mechanism.

The CFT model has been developed for spherical grains, whereas GAC has the form of small rods. However, the results clearly show that the removal mechanisms for sand filters and GAC filters are distinctly different. Where the removal of inorganic nanoparticles in sand filters increases in time, the removal in GAC filters clearly decreases, as shown in Fig. SI 5–S 13. Furthermore, it was noticed that in clean sand α_c increases for low doses of inorganic NPs, whereas in pre-loaded sand α_c increases for higher doses of inorganic NPs. Thus, α_c seems to be affected by the concentration, but the actual effect also depends on the state of the filter.

For both filter materials, the elution phase was accompanied by a sharp decline of nanoplastics detected in the effluent. The nanoplastics were thus well attached and retained by the column, which is in accordance with findings reported in literature for sand or glass bead-packed columns (Chu *et al.* 2019,²⁸ Molnar *et al.* 2015,⁵⁰ Pradel *et al.* 2020 (ref. 30)). An exception to this is given by the smaller carboxylated nanoplastics during GAC filtration which got mobilized again during elution phase leading to increasing NPs concentrations in the effluent (Fig. SI 14,[†] lower plot). Applying high energy sonication to the GAC grains resulted in the pulverization of the material, and thus in light scattering. As a result only a value ‘indicatively low’ could be attributed. For the experiments with nAu/nAg in virgin GAC fed with demineralized water hardly any ATP can be observed, whereas in virgin GAC with Leiduin water the ATP content of the GAC increases, caused by the water. For pre-loaded GAC, applying a high dose of NPs, a decrease in ATP-content was observed, which is in accordance with the results obtained for sand, reported above.

Apart from α_c also the single contactor removal efficiency η was determined for both inorganic NPs and nanoplastics, as shown in Table 5. Also for η no significant difference can be observed between nAu and nAg. In pre-loaded sand η appears to be higher than in clean sand, also indicating the positive effect of the presence of biomass. This effect is smaller for low doses of NPs than for high doses of NPs. For the 200 nm nanoplastics η values are lower than the η values obtained with inorganic NPs (also see Tables SI 8 and SI 9[†]). The effect of charge is clearly reflected in the value of η for the 200 nm particles, the plain particles showing a significantly higher η value. However, for the 50 nm particles the opposite effect can be observed, which reflects the contribution of charge interactions for smaller NPs. For the charged 50 nm nanoplastics η values are similar to the values obtained for the also negatively charged inorganic particles of the same size. The values of η in case of GAC are higher than the values obtained for sand, and the values of virgin GAC are

higher than those of pre-loaded GAC. However, remarkably the η values for the nanoplastics appear to be about ten times lower than those for the inorganic NPs.

In the ESI[†] (Table SI 9[†]) it is shown how the characterization of column materials can affect the values for η and α_c .

Transferability to real-scale drinking water treatment plants (DWTP)

Most of the DWTPs in the Netherlands operate at least these three purification techniques in sequence. At the full-scale treatment of Waternet a time of 20 min is applied for the coagulation/flocculation process, and 8 hours for sedimentation. Based on Fig. 3, where the maximum total time was 100 min, in theory total NPs cumulative removal rates between approximately 80–95% could then be expected based on the present findings. This is comparable to experimental findings by Donovan, Adams¹² reporting an almost complete removal of nAu, nAg and nTiO₂ particles during drinking water production. For nanoplastics of similar size and charge similar results are obtained as for inorganic NPs. For small NPs the charge seems to play a crucial role. For larger NPs another mechanism is involved, in which particle size seems to be more important. The removal rates presented here, however, were determined under specific laboratory conditions and should thus be used as a first indication only, although realistic conditions and settling times were applied. As shown above the loading of filter materials and the presence of NOM in the water matrix play a crucial role in the removal of NPs, which is in accordance with findings of.⁵⁷

Conclusions

Experiments were carried out in demineralized water and surface water. The surface water also was treated with an anion or cation exchange resin, to alter the water composition. CFS can effectively remove nAu, but is affected by the presence of NOM, Ca²⁺ and Mg²⁺. Higher NOM contents will result in lower removal rates. 60% of nAu was removed at a dosage of 4.5 mg L⁻¹ FeCl₃. Removal of 66% of the NOM prior to the CFS process increased the nAu removal by about 20%, under the test conditions. This was explained by charge interactions as both NOM and nAu were negatively charged. Removal of cations (Ca²⁺ and Mg²⁺) resulted in negligible nAu removal, showing that their presence is essential for the removal of nanoparticles from water. For nanoplastics it was shown that during CFS larger NPs (200 nm) are removed more efficiently than smaller NPs (50 nm), irrespective of their surface charge.

Column experiments were carried out with two types of pretreated surface water. Both sand and GAC filtration can remove NPs from water. However, for both filter materials the removal is based on different mechanisms. Where sand that has been used before (and thus has been loaded with *e.g.* NOM) results in an increased removal rate, loading of

GAC will give the opposite result. For nanoplastics it was found that a better removal can be obtained by GAC filtration than by sand filtration.

None of the processes studied here could remove all NPs, neither the metallic ones nor the plastics, from water. Future research is required to elucidate to what extent these experimental findings can be transferred to actual drinking water production, and what removal rates can be achieved by combination and optimization of processes. A better understanding of the effects of *e.g.* type and shape of the NPs will be required for this.

Conflicts of interest

There are no conflicts to declare.

Acknowledgements

Part of this research was carried out within the Joint Research Program of the Dutch Drinking Water Companies and the Belgian The Watergroup, and by the Dutch Technology Foundation TTW (Technologies for Risk Assessment of MicroPlastics, TRAMP project number 13940).

References

- G. E. Batley, J. K. Kirby and M. J. McLaughlin, Fate and risks of nanomaterials in aquatic and terrestrial environments, *Acc. Chem. Res.*, 2013, **46**(3), 854–862.
- C. O. Hendren, A. R. Badireddy, E. Casman and M. R. Wiesner, Modeling nanomaterial fate in wastewater treatment: Monte Carlo simulation of silver nanoparticles (nano-Ag), *Sci. Total Environ.*, 2013, **449**, 418–425.
- V. Stone, B. Nowack, A. Baun, N. van den Brink, F. von der Kammer, M. Dusinska, R. Handy, S. Hankin, M. Hassellöv, E. Joner and T. F. Fernandes, Nanomaterials for environmental studies: Classification, reference material issues, and strategies for physico-chemical characterisation, *Sci. Total Environ.*, 2010, **408**(7), 1745–1754.
- V. S. Sousa and M. Ribau Teixeira, Metal-based engineered nanoparticles in the drinking water treatment systems: A critical review, *Sci. Total Environ.*, 2020, **707**, 136077.
- R. Kaegi, A. Voegelin, C. Ort, B. Sinnet, B. Thalmann, J. Krismer, H. Hagendorfer, M. Elumelu and E. Mueller, Fate and transformation of silver nanoparticles in urban wastewater systems, *Water Res.*, 2013, **47**(12), 3866–3877.
- P. Westerhoff, A. Atkinson, J. Fortner, M. S. Wong, J. Zimmerman, J. Gardea-Torresdey, J. Ranville and P. Herckes, Low risk posed by engineered and incidental nanoparticles in drinking water, *Nat. Nanotechnol.*, 2018, **13**(8), 661–669.
- K. Kettler, K. Veltman, D. van de Meent, A. van Wezel and A. J. Hendriks, Cellular uptake of nanoparticles as determined by particle properties, experimental conditions, and cell type, *Environ. Toxicol. Chem.*, 2014, **33**(3), 481–492.
- R. Grillo, A. H. Rosa and L. F. Fraceto, Engineered nanoparticles and organic matter: A review of the state-of-the-art, *Chemosphere*, 2015, **119**, 608–619.
- B. M. Angel, G. E. Batley, C. V. Jarolimek and N. J. Rogers, The impact of size on the fate and toxicity of nanoparticulate silver in aquatic systems, *Chemosphere*, 2013, **93**(2), 359–365.
- C. O. Hendren, M. Lowry, K. D. Grieger, E. S. Money, J. M. Johnston, M. R. Wiesner and S. M. Beaulieu, Modeling approaches for characterizing and evaluating environmental exposure to engineered nanomaterials in support of risk-based decision making, *Environ. Sci. Technol.*, 2013, **47**(3), 1190–1205.
- F. Gottschalk, T. Sun and B. Nowack, Environmental concentrations of engineered nanomaterials: Review of modeling and analytical studies, *Environ. Pollut.*, 2013, **181**, 287–300.
- A. R. Donovan, C. D. Adams, Y. Ma, C. Stephan, T. Eichholz and H. Shi, Single particle ICP-MS characterization of titanium dioxide, silver, and gold nanoparticles during drinking water treatment, *Chemosphere*, 2016, **144**, 148–153.
- R. J. B. Peters, G. van Bommel, N. B. L. Milani, G. C. T. den Hertog, A. K. Undas, M. van der Lee and H. Bouwmeester, Detection of nanoparticles in Dutch surface waters, *Sci. Total Environ.*, 2018, **621**, 210–218.
- A. A. Markus, J. R. Parsons, E. W. M. Roex, G. C. M. Kenter and R. W. P. M. Laane, Predicting the contribution of nanoparticles (Zn, Ti, Ag) to the annual metal load in the Dutch reaches of the Rhine and Meuse, *Sci. Total Environ.*, 2013, **456–457**, 154–160.
- P. S. Bäuerlein, E. Emke, P. Tromp, J. A. M. H. Hofman, A. Carboni, F. Schooneman, P. de Voogt and A. P. van Wezel, Is there evidence for man-made nanoparticles in the Dutch environment?, *Sci. Total Environ.*, 2017, **576**, 273–283.
- H. J. C. van Dijk, J. Q. J. C. Verberk and P. J. de Moel, *Drinking water: principles and practices*, World Scientific Publishing Company, Singapore, 2006.
- T. E. Abbott Chalew, G. S. Ajmani, H. Huang and K. J. Schwab, Evaluating nanoparticle breakthrough during drinking water treatment, *Environ. Health Perspect.*, 2013, **121**(10), 1161–1166.
- A. A. Koelmans, N. H. Mohamed Nor, E. Hermsen, M. Kooi, S. M. Mintenig and J. De France, Microplastics in freshwaters and drinking water: Critical review and assessment of data quality, *Water Res.*, 2019, **155**, 410–422.
- S. M. Mintenig, M. Kooi, M. W. Erich, S. Primpke, P. E. Redondo-Hasselerharm, S. C. Dekker, A. A. Koelmans and A. P. van Wezel, A systems approach to understand microplastic occurrence and variability in Dutch riverine surface waters, *Water Res.*, 2020, **176**, 115723.
- L. Mughini-Gras, R. Q. J. van der Plaats, P. W. J. J. van der Wielen, P. S. Bauerlein and A. M. de Roda Husman, Riverine microplastic and microbial community compositions: A field study in the Netherlands, *Water Res.*, 2021, **192**, 116852.
- L. M. Hernandez, N. Yousefi and N. Tufenkji, Are there nanoplastics in your personal care products?, *Environ. Sci. Technol. Lett.*, 2017, **4**(7), 280–285.
- J. Gigault, B. Pedrono, B. Maxit and A. Ter Halle, Marine plastic litter: The unanalyzed nano-fraction, *Environ. Sci.: Nano*, 2016, **3**(2), 346–350.

- 23 A. Ter Halle, L. Jeanneau, M. Martignac, E. Jardé, B. Pedrono, L. Brach and J. Gigault, Nanoplastic in the North Atlantic Subtropical Gyre, *Environ. Sci. Technol.*, 2017, **51**(23), 13689–13697.
- 24 A. Wahl, C. Le Juge, M. Davranche, H. El Hadri, B. Grassl, S. Reynaud and J. Gigault, Nanoplastic occurrence in a soil amended with plastic debris, *Chemosphere*, 2021, **262**, 127784.
- 25 M. Pivokonský, L. Pivokonská, K. Novotná, L. Čermáková and M. Klimtová, Occurrence and fate of microplastics at two different drinking water treatment plants within a river catchment, *Sci. Total Environ.*, 2020, **741**, 140236.
- 26 Z. Wang, T. Lin and W. Chen, Occurrence and removal of microplastics in an advanced drinking water treatment plant (ADWTP), *Sci. Total Environ.*, 2020, **700**, 134520.
- 27 J. Hou, X. Xu, L. Lan, L. Miao, Y. Xu, G. You and Z. Liu, Transport behavior of micro polyethylene particles in saturated quartz sand: Impacts of input concentration and physicochemical factors, *Environ. Pollut.*, 2020, **263**, 114499.
- 28 X. Chu, T. Li, Z. Li, A. Yan and C. Shen, Transport of microplastic particles in saturated porous media, *Water*, 2019, **11**(12), 2474.
- 29 W. Zhao, P. Zhao, Y. Tian, C. Shen, Z. Li, P. Peng and C. Jin, Investigation for Synergies of Ionic Strength and Flow Velocity on Colloidal-Sized Microplastic Transport and Deposition in Porous Media Using the Colloidal-AFM Probe, *Langmuir*, 2020, **36**(22), 6292–6303.
- 30 A. Pradel, H. E. Hadri, C. Desmet, J. Ponti, S. Reynaud, B. Grassl and J. Gigault, Deposition of environmentally relevant nanoplastic models in sand during transport experiments, *Chemosphere*, 2020, **255**, 126912.
- 31 R. Lehner, C. Weder, A. Petri-Fink and B. Rothen-Rutishauser, Emergence of Nanoplastic in the Environment and Possible Impact on Human Health, *Environ. Sci. Technol.*, 2019, DOI: [10.1021/acs.est.8b05512](https://doi.org/10.1021/acs.est.8b05512).
- 32 R. Floris, Removal of engineered nanoparticles in drinking water treatment processes., in *Membrane Science and Technology*, University of Twente: Enschede, the Netherlands, 2017.
- 33 Q. Sun, Y. Li, T. Tang, Z. Yuan and C. P. Yu, Removal of silver nanoparticles by coagulation processes, *J. Hazard. Mater.*, 2013, **261**, 414–420.
- 34 H. Wang, J. Qi, A. A. Keller, M. Zhu and F. Li, Effects of pH, ionic strength and humic acid on the removal of TiO₂ nanoparticles from aqueous phase by coagulation, *Colloids Surf., A*, 2014, **450**(1), 161–165.
- 35 R. J. Honda, V. Keene, L. Daniels and S. L. Walker, Removal of TiO₂ nanoparticles during primary water treatment: Role of coagulant type, dose, and nanoparticle concentration, *Environ. Eng. Sci.*, 2014, **31**(3), 127–134.
- 36 N. Kinsinger, R. Honda, V. Keene and S. L. Walker, Titanium dioxide nanoparticle removal in primary prefiltration stages of water treatment: Role of coating, natural organic matter, source water, and solution chemistry, *Environ. Eng. Sci.*, 2015, **32**(4), 292–300.
- 37 R. Floris, G. Moser, K. Nijmeijer and E. R. Cornelissen, Effect of multicomponent fouling during microfiltration of natural surface waters containing C₆₀ fullerene nanoparticles, *Environ. Sci.: Water Res. Technol.*, 2017, **3**(4), 744–756.
- 38 R. Floris, K. Nijmeijer and E. R. Cornelissen, Removal of aqueous C₆₀ fullerene from water by low pressure membrane filtration, *Water Res.*, 2016, **91**, 115–125.
- 39 L. Ramirez Arenas, S. Ramseier Gentile, S. Zimmermann and S. Stoll, Fate and removal efficiency of polystyrene nanoplastics in a pilot drinking water treatment plant, *Sci. Total Environ.*, 2022, **813**, 152623.
- 40 L. Ramirez Arenas, S. Ramseier Gentile, S. Zimmermann and S. Stoll, Nanoplastics adsorption and removal efficiency by granular activated carbon used in drinking water treatment process, *Sci. Total Environ.*, 2021, **791**, 148175.
- 41 L. Ramirez Arenas, S. Ramseier Gentile, S. Zimmermann and S. Stoll, Coagulation of TiO₂, CeO₂ nanoparticles, and polystyrene nanoplastics in bottled mineral and surface waters. Effect of water properties, coagulant type, and dosage, *Water Environ. Res.*, 2020, **92**(8), 1184–1194.
- 42 P. H. A. Timmers, T. Slootweg, A. Knezev, M. van der Schans, L. Zandvliet, A. Reus, D. Vughs, L. Heijnen, T. Knol, J. El Majjaoui, P. van der Wielen, P. J. Stuyfzand and K. Lekkerkerker-Teunissen, Improved drinking water quality after adding advanced oxidation for organic micropollutant removal to pretreatment of river water undergoing dune infiltration near The Hague, Netherlands, *J. Hazard. Mater.*, 2022, **429**, 128346.
- 43 WHO, Drinking Water Parameter Cooperation Project: Support to the revision of Annex I Council Directive 98/83/EC on the Quality of Water Intended for Human Consumption (Drinking Water Directive), WHO, Editor. 2017, World Health Organization: Geneva.
- 44 M. Shen, B. Song, Y. Zhu, G. Zeng, Y. Zhang, Y. Yang, X. Wen, M. Chen and H. Yi, Removal of microplastics via drinking water treatment: Current knowledge and future directions, *Chemosphere*, 2020, **251**, 126612.
- 45 Y. Zhang, A. Diehl, A. Lewandowski, K. Gopalakrishnan and T. Baker, Removal efficiency of micro- and nanoplastics (180 nm–125 μm) during drinking water treatment, *Sci. Total Environ.*, 2020, **720**, 137383.
- 46 N. Toride, F. J. Leij and M. T. van Genuchten, The CXTFIT Code for Estimating Transport Parameters from Laboratory or Field Tracer Experiments; version 2.0., Salinity Laboratory, Riverside CA, USA, 1995.
- 47 K. M. Yao, M. T. Habibian and C. R. O'Melia, Water and Waste Water Filtration: Concepts and Applications, *Environ. Sci. Technol.*, 1971, **5**(11), 1105–1112.
- 48 B. Berkowitz, I. Dror and B. Yaron, Contaminant geochemistry: Interactions and transport in the subsurface environment: Second edition, *Contaminant Geochemistry: Interactions and Transport in the Subsurface Environment*, 2nd edn, 2014, vol. 9783642547775, pp. 1–577.
- 49 N. Tufenkji and M. Elimelech, Correlation Equation for Predicting Single-Collector Efficiency in Physicochemical Filtration in Saturated Porous Media, *Environ. Sci. Technol.*, 2004, **38**(2), 529–536.

- 50 I. L. Molnar, W. P. Johnson, J. I. Gerhard, C. S. Willson and D. M. O'Carroll, Predicting colloid transport through saturated porous media: A critical review, *Water Resour. Res.*, 2015, **51**(9), 6804–6845.
- 51 M. Enfrin, L. F. Dumée and J. Lee, Nano/microplastics in water and wastewater treatment processes – Origin, impact and potential solutions, *Water Res.*, 2019, **161**, 621–638.
- 52 A. Matilainen, M. Vepsäläinen and M. Sillanpää, Natural organic matter removal by coagulation during drinking water treatment: A review, *Adv. Colloid Interface Sci.*, 2010, **159**(2), 189–197.
- 53 K. Novotna, L. Cermakova, L. Pivokonska, T. Cajthaml and M. Pivokonsky, Microplastics in drinking water treatment – Current knowledge and research needs, *Sci. Total Environ.*, 2019, **667**, 730–740.
- 54 Y. Han, G. Hwang, D. Kim, S. A. Bradford, B. Lee, I. Eom, P. J. Kim, S. Q. Choi and H. Kim, Transport, retention, and long-term release behavior of ZnO nanoparticle aggregates in saturated quartz sand: Role of solution pH and biofilm coating, *Water Res.*, 2016, **90**, 247–257.
- 55 H. Jian-Zhou, L. Cheng-Cheng, W. Deng-Jun and D. M. Zhou, Biofilms and extracellular polymeric substances mediate the transport of graphene oxide nanoparticles in saturated porous media, *J. Hazard. Mater.*, 2015, **300**, 467–474.
- 56 J. Pulit, M. Banach, R. Szczygłowska and M. Bryk, Nanosilver against fungi. Silver nanoparticles as an effective biocidal factor, *Acta Biochim. Pol.*, 2013, **60**(4), 795–798.
- 57 A. J. Pelley and N. Tufenkji, Effect of particle size and natural organic matter on the migration of nano- and microscale latex particles in saturated porous media, *J. Colloid Interface Sci.*, 2008, **321**(1), 74–83.
- 58 M. Lapointe, J. M. Farner, L. M. Hernandez and N. Tufenkji, Understanding and Improving Microplastic Removal during Water Treatment: Impact of Coagulation and Flocculation, *Environ. Sci. Technol.*, 2020, **54**(14), 8719–8727.